Chemosphere 293 (2022) 133410

Contents lists available at ScienceDirect

Chemosphere

journal homepage: www.elsevier.com/locate/chemosphere

Targeted and untargeted metabolomic analysis of *Procambarus clarkii* exposed to a "chemical cocktail" of heavy metals and diclofenac

G. Rodríguez-Moro [a], C. Román-Hidalgo [b], S. Ramírez-Acosta [a], N. Aranda-Merino [b], J. L. Gómez-Ariza [a,1], N. Abril [c,1], M.A. Bello-López [b,1], R. Fernández-Torres [b,**,1], T. García-Barrera [a,*,1]

[a] Research Center for Natural Resources, Health and the Environment (RENSMA). Department of Chemistry, Faculty of Experimental Sciences, University of Huelva, Fuerzas Armadas Ave., 21007, Huelva, Spain
[b] Department of Analytical Chemistry, Faculty of Chemistry, Universidad de Sevilla, 41012, Sevilla, Spain
[c] Department of Biochemistry and Molecular Biology, University of Córdoba, Campus de Rabanales, Edificio Severo Ochoa, E-14071, Córdoba, Spain

HIGHLIGHTS

- Untargeted and targeted metabolomics was applied to *Procambarus clarkii*.
- An analytical platform based on the use of organic and inorganic MS is proposed.
- Metabolic impairments caused by As, Cd and DCF are described for the first time.
- Bioaccumulation in tissues was determined along several exposure times.

GRAPHICAL ABSTRACT

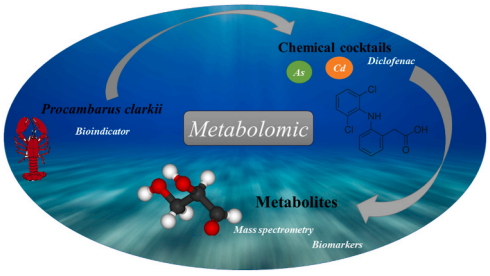

ARTICLE INFO

Handling Editor: Magali Houde

Keywords:
Procambarus clarkii
Chemical cocktails
Metabolomics
Mass spectrometry
Biomarkers

ABSTRACT

Water pollution poses an important problem, but limited information is available about the joined effects of xenobiotics of different chemical groups to evaluate the real biological response. *Procambarus clarkii (P. clarkii)* has been demonstrated to be a good bioindicator for assessing the quality of aquatic ecosystems. In this work, we studied the bioaccumulation of cadmium (Cd), arsenic (As) and diclofenac (DCF) in different tissues of *P. clarkii* during 21 days after the exposure to a "chemical cocktail" of As, Cd and DCF, and until 28 days considering a depuration period. In addition, a combined untargeted and targeted metabolomic analysis was carried out to delve the metabolic impairments caused as well as the metabolization of DCF. Our results indicate that As and Cd were mainly accumulated in the hepatopancreas followed by gills and finally abdominal muscle. As and Cd show a general trend to increase the concentration throughout the exposure experience, while a decrease in the concentration of these elements is observed after 7 days of the depuration process. This is also the case in the abdominal muscle for Cd, but not for As and DCF, which increased the concentration in this tissue in the depuration phase. The hepatopancreas showed the greatest number of metabolic pathways affected. Thus, we observed a crucial bioaccumulation of xenobiotics and impairments of metabolites in different tissues. This is the

* Corresponding author.
** Corresponding author.
E-mail addresses: rutft@us.es (R. Fernández-Torres), tamara@dqcm.uhu.es (T. García-Barrera).
[1] Senior authors.

https://doi.org/10.1016/j.chemosphere.2021.133410
Received 5 October 2021; Received in revised form 17 December 2021; Accepted 21 December 2021
Available online 27 December 2021

first study combining the exposure to metals and pharmaceutically active compounds in *P. clarkii* by untargeted metabolomics including the biotransformation of DCF.

1. Introduction

The problem of environmental pollution due to the occurrence of pharmaceutically active compounds (PACs), organic pollutants or heavy metals in aquatic ecosystems has led to a growing interest about the study and use of biomarkers (Fernández-Cisnal et al., 2017, 2018; García-Sevillano et al., 2015; Hodson, 2002; Zhang et al., 2019, 2021). Likewise, aquatic invertebrates, among other organisms are very good bioindicators that result particularly useful for assessing the quality of aquatic ecosystems since they present a relationship between the content of contaminants in their tissues and in the environment (Hodson, 2002). The freshwater crayfish *P. clarkii* is an invasive foreign species in Spain, native of north-eastern Mexico and south-central USA that was spread around the world (HUNER, 1988). *P. clarkii* is considered an effective bioindicator of environmental pollution (Suárez-Serrano et al., 2010) and has been used for a wide number of studies related with the bioaccumulation of heavy metals (Fernández-Cisnal et al., 2017), Cd and Zn (Bini et al., 2015) and As or As species (Devesa et al., 2002; Gedik et al., 2017). Other studies have been related with the alteration of the metabolite profile since the exposure to stressors could modify the metabolic pathways for reproduction, growth and survival (Hines et al., 2010). Metabolomics is the study of the entirety metabolome, defined as the set of endogenous low molecular mass compounds (LMM). Since metabolic changes are the ultimate response of an organism to environmental stimuli, metabolomics is most predictive of the phenotype. Likewise, environmental metabolomics allows obtaining a global view of the metabolic fingerprint of biological systems exposed to contaminants, providing information at the same time about the interactions of contaminants with living organisms (García-Sevillano et al., 2015). Mass spectrometry techniques are widely used in metabolomics, usually coupled to gas chromatography (GC-MS), which is a robust tool that provides high sensitivity and good resolution for LMM metabolites (Pasikanti et al., 2008) or liquid chromatography (LC), for the simultaneous determination of metabolites with very diverse chemical nature, extending from metabolites detectable by GC-MS to non-volatile compounds, through the use of complementary retention mechanisms and ionization techniques (Kuehnbaum and Britz-Mckibbin, 2013).

Previous works described the metabolic impairments caused by environmental pollution (Fernández-Cisnal et al., 2018), food availability and dissolved oxygen concentration (Izral et al., 2018) in *P. clarkii* showing that environmental metabolomics is a powerful bioassesment tool capable of identifying ecological consequences of stressors. The effects of Cd on oxidative stress, histopathology and transcriptome changes (Zhang et al., 2019), microbiota (Zhang et al., 2020) and immunosuppression (Wei et al., 2020) have been reported, as well as the effects of DCF exposure on intestinal histology, antioxidant defense and microbiota (Zhang et al., 2021). However, although the synergistic and antagonistic interactions between elements have been extensively reviewed (García-Barrera et al., 2012), limited information is available about the effects of the exposure to joint environmental pollutants of different biochemical characteristics to assessment the effects in the environment (Van Genderen et al., 2015). DCF has been selected as a pharmaceutical model in this work because of its high potential to form metal complexes, which completely modifies its properties and may lead to the creation of other possible emerging contaminants (Lonappan et al., 2016).

In the present study, we investigated the metabolic impairments caused by a mixture of DCF, Cd and As at environmentally relevant concentrations to the crayfish *P. clarkii*. To this end, a combined targeted and untargeted metabolomic analytical multiplatform based on the use of quadrupole time of flight mass spectrometry (QTOF) with ultra-high performance LC (UPLC) and GC has been applied to establish alterations in metabolic pathways. The bioaccumulation of these xenobiotics and biotransformation of DCF have also been investigated in different tissues of *P. clarkii*.

2. Materials and methods

2.1. Animals, experimental design and dosage information

P. clarkii specimens were captured at the rice crops of Isla Mayor (Sevilla, Spain), using traps placed in the waterways and shipped to our laboratory under cool conditions (<4 °C). The crayfish were acclimated, in tanks with aerated and dechlorinated freshwater during 2 weeks before the beginning of the experiment.

DCF, $CdCl_2$ and As_2O_3 were purchased from Sigma Aldrich, Steinheim, Germany. Stock solutions were prepared in water to obtain a final nominal concentration in the exposure tank of 2 μg L^{-1} of $CdCl_2$ and As_2O_3 and 40 μg L^{-1} of DCF. These doses were selected as they are consistent with the concentrations previously observed in specimens sampled in the environment (Fernández-Cisnal et al., 2018; Lonappan et al., 2016) and also they are a compromise between semi-realistic conditions and concentrations that are expected to cause an effect. Crayfish were fed with fish feed pellets (Surtropic Company, Spain) and water of every tank was totally renewed every 48 h. Besides, natural 12 h light/dark photoperiods were set.

The experiment lasted 28 days (21 days of exposition and 7 additional days of depuration). To ensure exposure, the chemical cocktail was administered every two days, when the water of the tanks was renewed. Animals were separated into control group and treated group. Crayfish (ten animals per group and sampling time) were sampled at the start of the assay (0 days after acclimatization), after 10 and 21 days of exposure, and finally after 7 days of depuration (28 days after exposure). Hepatopancreas, antennal gland, gills, abdominal muscle and spinal nerve tissues were excised, cold in liquid nitrogen and stored at −80 °C. Additionally, crayfish mass and total length were measured prior to animals being sacrificed (7.7 ± 0.4 cm in length and 20.1 ± 2.3 g in wet weight).

Physicochemical water parameter values of temperature, conductivity, dissolved oxygen, pH, hardness and ions, measured every day during the assay varied little showing values of 17.8 ± 1.6 °C, 477.4 ± 30.5 μS/cm; 8.5 ± 0.8 mg/L O_2, 8.3 ± 0.2 for pH, 145 ± 3.7 mg/L $CaCO_3$, 0.6 ± 0.7 mg/L, NH_4^+, 4.1 ± 2.1 mg/L K^+, 0.5 ± 0.6 mg/L NO_2^-, 0.1 ± 0.1 mg/L NO_3^-, <0.2 mg/L PO_4^{3-}, 69.7 ± 15.7 mg/L Cl^- and 6.8 ± 1.7 mg/L SO_4^{2-}, respectively. Crayfish mortality was daily checked being lower than 2% (averaged).

2.2. Sample preparation for total metal concentration of cadmium and arsenic

Samples were individually homogenized using liquid nitrogen with a SEPX SamplepREP (ten strokes/second during 30s). The acid digestion for total metal determination was carried out using a microwave-accelerated reaction system model MARS (CEM Corporation, Matthews, NC, USA) as previously described (Rodríguez-Moro et al., 2020) and analysed by triple quadrupole inductively coupled plasma mass spectrometer (ICP-QQQ-MS) model Agilent 8800 Triple Quad (Agilent Technologies, Tokyo, Japan). TORT-2, crab hepatopancreas, was used as certified reference material to validate the analysis.

2.3. Sample preparation for diclofenac and metabolites analysis

To determine DCF and their metabolites a previous method was applied (Kazakova et al., 2018). In brief, 0.1 g of lyophilized tissue were extracted in microwave (Ethos One, Millestone, Sorisole (BG), Italy) at 50 W for 5 min using 2 mL of a mixture 1:1 (v/v) acetonitrile/water, 10 μL of proteinase-k and 1 μL of pure formic acid. Then, samples were centrifuged at 12,825 *g* for 10 min (20 min for hepatopancreas) at 4 °C, evaporated to dryness using a speed vacuum system and stored at −80 °C until analysis. The samples were reconstituted to 1 mL with 0.1% (v/v) formic acid aqueous solution and microfiltered (0.22 μm) prior to analysis.

2.4. Sample preparation for untargeted metabolomic analysis

After criohomogenization, metabolites were removed from tissues applying an optimized methodology (M. A. García-Sevillano et al., 2015). Before the analysis by UPLC-QTOF-MS, 100 μL of 1:1 (v/v) acetonitrile/water were added to the extracts and 10 μL were injected into the system.

Before GC-MS analysis, the extracted metabolites were derivatized following the protocol described in the literature (Begley et al., 2009). Finally, 1 μL of the supernatant was injected into the GC-MS in splitless mode.

Quality control samples (QC) were used throughout the analysis and were prepared adding the same volume of all samples of each group and were treated and analysed identically to the rest of the samples.

2.5. Diclofenac and metabolites determination

DCF and their hydroxylated metabolites quantification on abdominal muscle and hepatopancreas was performed using a previous methods with several modifications (Barreales-Suárez et al., 2018; Trombini et al., 2021). An Acquity® UPLC (Waters, Milford, MA, USA) coupled to a Xevo® G2S QTOF mass spectrometer (Waters, Micromass, Manchester, UK) was used. 10 μL of sample were injected into an Acquity® BEH C18 column (50 mm × 2.1 mm i. d, 1.7 μm) at 30 °C. For full mass analysis, the mobile phase consisted of water (A) and a methanolic solution of formic acid 0.1% (v/v) (B) at 0.3 mL min^{-1} for 17 min. Gradient elution was applied starting with an initial composition of 70% A, decreased to 45% A at 3 min and maintaned for 7 min. From 10 to 13 min, it changed to 10% A and returned to the initial conditions at 15 min and kept for 2 min. Detection was carried out within 50–800 *m/z*, with an ESI source at 2.0 kV capillary voltage, cone voltage 40 V and source and desolvation temperatures of 120 °C and 400 °C, respectively. The nebulization gas and cone gas (N_2) were set at 600 L h^{-1} and 30 L h^{-1}, respectively. Under these conditions recoveries obtained for DCF were (85 ± 3.6) % for hepatopancreas and (90 ± 4.8) % for abdominal muscle.

Besides quantification, a target search of DCF metabolites was also carried out using ESI^+ and ESI^- polarities. Gradient elution started at 90% A, decreasing to 5% A in 17 min, returning to initial conditions at 18 min and keeping for 2 min before the following injection. UPLC–QTOF-MS detection collects data within 50–800 *m/z* using two scan functions that provides fragment ion information without precursor ion selection. Thus, two functions were acquired at different collision energies: a low energy function obtained at 2 eV; and a high-energy function obtained using a collision energy ramp ranging from 15 to 30 eV.

Data acquisition were performed using a reference spray (lockSpray®) to certify accuracy and reproducibility. Leucine Enkephalin (200 pg μL^{-1} in acetonitrile/0.1% aqueous formic acid 1:1 v/v) was used as the reference mass (*m/z* $[M+H]^+$ 556.2771 and *m/z* $[M-H]^-$ 554.2615) at a flow rate of 10 μL min^{-1}. The lockSpray® frequency was set at 30 s (every 30 s the flow from the lockSpray® needle was introduced into the mass spectrometer for 0.30 s) to mass correction of the analyte. The lockSpray® capillary was set at 2.54 KV.

MassLynx® version 4.1 software was used as data process, while metabolites were identified using Cromalynx® XS (Waters, Micromass, Manchester, UK) which identifies metabolites previously defined. In this case a target search of 46 candidates was realized based on previous metabolites reported in bibliography (Wilson et al., 2018). The identification was based on exact mass (error <5 ppm), the isotopic pattern of chlorine (Cl) and the MS/MS fragments obtained in the second function by comparison with that reported previously in literature.

2.6. Untargeted metabolomic fingerprinting

2.6.1. UPLC-ESI-QTOF-MS analysis, data processing and metabolite identification

UPLC-QTOF-MS experiments were performed using an Agilent 6550 iFunnel Q-TOF LC/MS System (Agilent Technologies, Tokyo, Japan) coupled to an Agilent 1290 Series LC pump with a reversed phase chromatography using the methodology described by Xiong et al. (2018). Briefly, 10 μL of the extract were placed into an autosampler maintained at 4 °C and injected into an Acquity® HSS T3 column (100 mm × 2.1 mm, 1.8 μm) at 40 °C. The mobile phase flow was set at 0.2 mL min^{-1} with solvent A (0.1% (v/v) formic acid in water) and solvent B (0.1% (v/v) formic acid in acetonitrile). Metabolites were separated using the following gradient conditions: 100% of solvent A for 0.5 min, decreased to 5% A in 20 min, maintained for 1 min and returned to the initial conditions in 24 min. For the period of the analysis, two reference masses were constantly infused into the system for mass correction in both ionization modes: *m/z* 121.0509 and 922.0098 for ESI^+ and *m/z* 112.9856 and 1033.9881 for ESI^-. The optimized parameters of the system were as follows: full-scan mode from 50 to 1100 *m/z*, drying gas flow rate 12 L min^{-1} at 250 °C, capillary voltage set at 3 KV, gas nebulizer 52 psi, fragmentor voltage: 175 V for ESI^+ and 250 V for ESI^-, skimmer voltage 65 V and octopole radio frequency voltage 750 V.

The data pre-processing was performed with the software Mass Profinder® version B.10.00. The Mass Profinder® contains different molecular features extraction (MFE) algorithms to develop the steps for pre-processing, including the peak picking and peak alignment step. Data obtained were imported to Mass Profiler® Professional (MPP) B.8.00 to achieve univariate and multivariate analysis. An unsupervised Principal Component Analysis (PCA) was performed to supervise the trend of QCs samples with the purpose of evaluating the stability and reliability of the metabolomic study. Finally, differences among the groups were investigated by partial least square discriminant analysis (PLS-DA) and the quality of the built models was determined with the values of R^2 and Q^2 provided by the software (indicative of class separation and predictive power of the model, respectively). The identity of compounds was confirmed by METLIN and LC-MS/MS experiments, with the same chromatographic conditions. Moreover, differences among the three times of exposure in each tissue were evaluated for each individual metabolite using one-way ANOVA ($p < 0.05$) followed by Post hoc Tukey's *t*-test. Finally, the false discovery rate at level α 0.05 was checked by Benjamini-Hochberg correction.

2.6.2. GC-EI-MS analysis

Metabolomic analysis by GC-MS was carried out using a Factor Four column VF-5MS (30 m × 0.25 μm ID, 0.25 μm film thickness) into a Trace GC ULTRA gas chromatograph coupled to an ITQ900 ion trap mass spectrometer detector (Thermo Fisher Scientific). The analyses were carried out in full scan mode with the mass range of 40–650 *m/z* and ionization by electronic impact (EI) with a voltage of 70eV. The temperature of injector was maintained at 280 °C, using helium as carrier gas (1 mL min^{-1}). The chromatographic method was: the column temperature was set at 100 °C for 0.5 min, and then increased to 320 °C at 15 °C min^{-1}, and finally hold for 7 min.

Data processing from GC-MS was carried out with R platform based free access XCMS software. The XCMS parameters were optimized to extract the maximum information as possible. Finally, the settings

applied were: S/N threshold 2, full width at half-maximum (fwhm) 3, and width of the *m/z* range 0.1 (step parameter). After peak extraction, grouping and retention time correction of peaks (alignment) was accomplished in three iterative cycles with descending bandwidth (bw) from 5 to 1 s.

The data matrix obtained, including the resulting abundances of each metabolite, was processed with SIMCA-P software (version 11.5, published by UMetrics AB, Umeå, Sweden) to achieve partial least-squares discriminant analysis (PLS-DA) with the aim of finding significant differences between the studied groups.

For GC-MS, the commercial library NIST Mass Spectral Library, was used to the annotation the unknown compounds, agreed only those metabolites that had a spectrum score higher 80%. The Kovat's retention indices of the compounds were also determined using a n-alkane mix (from C10 to C40, Sigma Aldrich, Germany). In our study, the metabolites were identified to MSI (Metabolomics Standards Initiative) as Level 2 (Sumner et al., 2007).

2.6.3. Pathway analysis

To identify the most significant pathways in relation to altered metabolites after As, Cd and DCF exposure in different studied organs, Metaboanalyst 5.0 (https://www.metaboanalyst.ca/) was performed. The library selected was "*Danio rerio*" zebrafish using the algorithms *Hypergeometric Test* for pathway enrichment and *Relative-Betweenness Centrality* for pathway topological analysis.

3. Results

Herein we describe a nontargeted metabolomic methodology, based on the combination of two complementary analytical techniques, to investigate the metabolic damages caused by a chemical cocktail of As, Cd and DCF in the crayfish *P. clarkii* (hepatopancreas, antennal gland, gills, abdominal muscle and spinal nerve). Moreover, targeted metabolomics was applied to examine the effects of the exposure on the uptake, distribution and metabolism of DCF in samples of abdominal muscle and hepatopancreas.

3.1. Bioaccumulation of contaminants in different tissues

As and Cd concentrations were quantified by ICP-QQQ-MS in important metabolic organs (hepatopancreas, abdominal muscle and gills) of crayfish *P. clarkii* and the results are presented in Table S1 and in Fig. 1.

As and Cd accumulated in hepatopancreas and gills along the exposure time and their concentration decreased after the 7-days deputation period. The maximum concentration of As was similar in both organs, but Cd reached concentrations two fold higher in hepatopancreas than in gills. A similar pattern was observed for Cd in the abdominal muscle, but the maximum concentration was 50 times lower than that of the hepatopancreas. However, As showed a quite different pattern in abdominal muscle, with concentrations significantly lower than control crayfish during the exposure period and almost doubling the control after depuration.

Water in the housing tanks was renewed every 48 h and samples

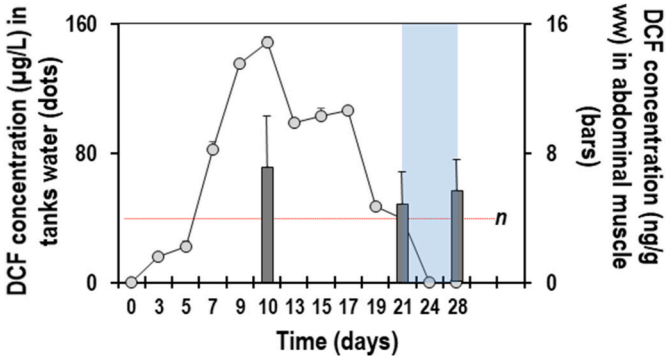

Fig. 2. Concentration of DCF (dots) in the tank water and the abdominal muscle (bars) of *P. clarkii* along the experimental time. Water from the tanks was renewed every 48 h and DCF concentration measured just before renewing. The purification period is marked in blue. (For interpretation of the references to colour in this figure legend, the reader is referred to the Web version of this article.)

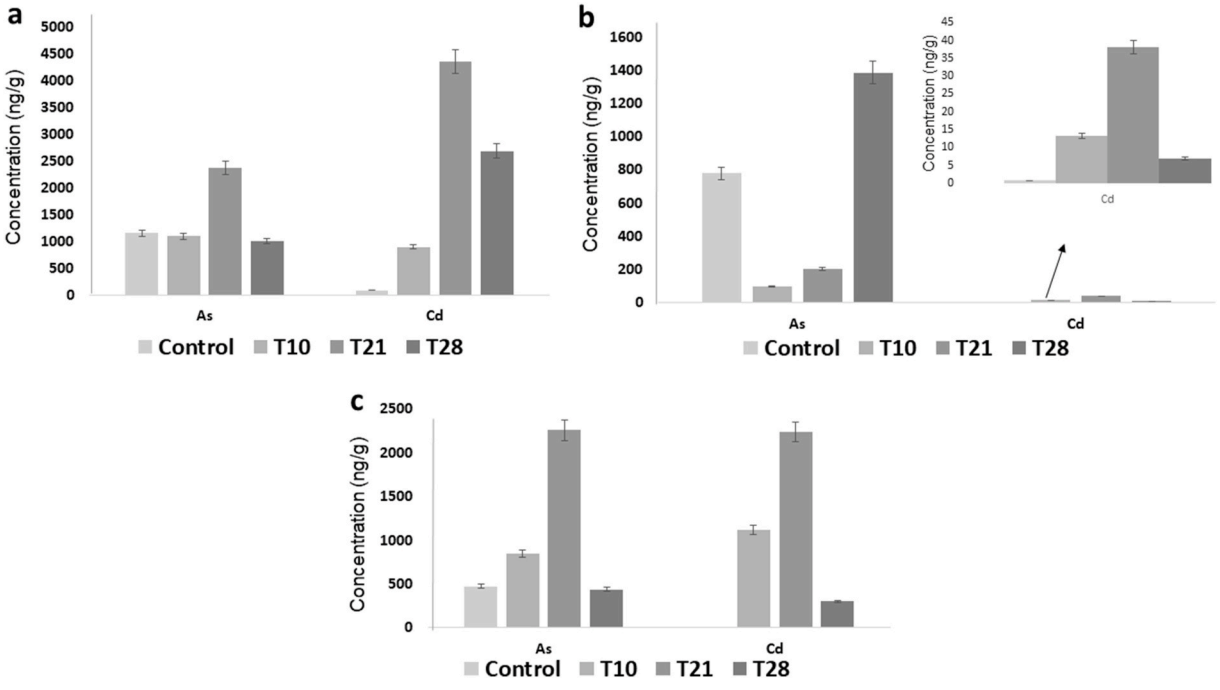

Fig. 1. Bioaccumulation of As and Cd in: a) hepatopancreas; b) abdominal muscle and c) gills of *P. clarkii* along the exposure experiment.

collected just before renewing to determine the DCF concentration in the water (Fig. 2, Table S2), in order to compare the nominal concentration versus measured concentration along the exposure survey. Data in Fig. 2 and Table S2 show that DCF concentration in water decreased 13–60% during the first five days of the survey, but then increased to almost 3 times the nominal value on day 10 and remained at 3 times the nominal value until day 15, to finally remain close to the nominal concentration until day 21 of exposure. During the purification phase (days 22–28), non-quantifiable levels of DCF were found in the analysed water, but the compound was detected in all the water samples, which indicates the organisms suffer a depuration process during this phase of the survey.

All but one (with 1.35 ± 0.21 ng g^{-1} wet weigh at 21 day) crayfish were free of DCF in their hepatopancreas at any time (Table S2) and bioaccumulation of DCF occurred at very low levels in the abdominal muscle. The bioconcentration factor (BCF) was calculated at 10 (BCF_{10}) and 21 (BCF_{21}) days as the ratio between the analyte concentration in the tissue and in the exposure water. The obtained BCF_{10} and BCF_{10} values, 0.17 ± 0.26 and 0.11 ± 0.12 respectively, demonstrate no relevant bioconcetrations of DCF in the abdominal muscle of this arthropod as according to regulatory thresholds established in Regulation (EC) No 1907/2006 (REACH), PACs with a high potential for bioaccumulation have BCF >1000 and log Kow >3 (*European Commission Regulation (EC) No 1907/2006*). These low bioconcentrations have been previously reported in fish specimens (Memmert et al., 2013), attributing the behavior to the chemical properties of DCF due to its ionizable character (pKa of 3.99–4.16), and its octanol-water distribution coefficient ($logK_D$ within 1.3–1.9).

3.2. Untargeted metabolomics

After data processing, PLS-DA showed significantly separated clusters among exposed groups *versus* control in each tissue at the different days of the exposure, except for the hepatopancreas and spinal nerve by UPLC-QTOF-MS (ESI^-). The PLS-DA obtained by UPLC-QTOF-MS (ESI^- and ESI^+) and GC-MS are shown in Figs. S1 and S2, respectively. Moreover, Table S3 shows the values of R^2 and Q^2 of PLS-DA score plot for UPLC-QTOF-MS and GC-MS analysis in individual organs.

As can be seen in Figs. S1 and S2, *P. clarkii* undergoes metabolic disorders promoted by the "chemical cocktail" in all the tissues and the clusters are well differentiated. Metabolites with statistically significant difference among the groups are shown in Tables S4, S5, S6, S7, S8. Moreover, Tables S9 and S10 show fragments obtained in the MS/MS identification of the metabolites for LC-MS/MS and GC-MS. Moreover, a heatmap summarizing the significant metabolites altered in hepatopancreas is shown in Fig. 3.

Fig. 4 shows the number of significant compounds that have been found to be common or uncommon on the different days in different tissue.

The highest number of altered metabolites were obtained after 28 days of the exposure for all the tissues studied, except for abdominal muscle where the highest number was found after 21 days. Hence, this exposure time was selected to illustrate (Fig. 5) the number of common significant metabolites between the different tissues. As can be seen, the "chemical cocktail" caused different metabolic impairments in the various analysed tissues, and only a little number of metabolites are independent of tissue and experimental conditions.

Our results also showed interrelations between metals and metabolites as can be seen in the spearman correlation heatmap (Fig. S3). Likewise, Cd significantly correlates with 7 metabolites (possitive and negative), but As only with 1, positively. These metabolites belongs to carboximidic acids, fatty acyls, glycerolipids, glycerophospholipids, Sphingolipids and unsaturated hydrocarbons.

The Metaboanalyst 4.0 web tool was used to identify the most significant pathways altered by the exposure to the "chemical cocktail". The exposure time T28 was selected in this analysis since, as previously explained, a greater number of metabolites were found to be altered in most tissues. The most significantly altered pathways in each tissue are represented in Fig. 6. The hepatopancreas showed the greatest number of metabolic pathways affected followed by gills, abdominal muscle, antennal gland and spinal nerve.

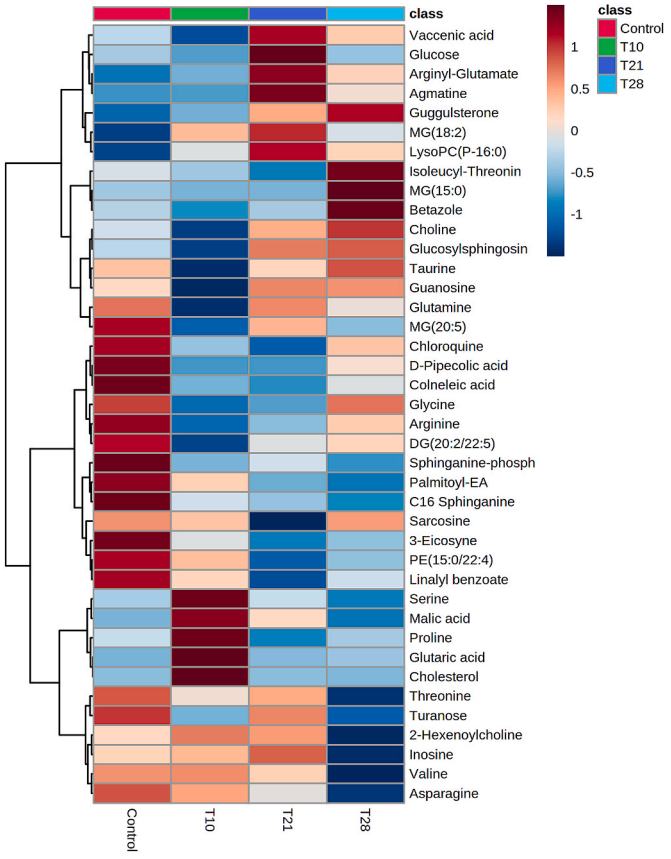

Fig. 3. Heatmap showing significant metabolites altered in hepatopancreas of *P. clarkii* after As, Cd and DCF co-exposure at different times. DG: diacylglycerol; MG: Monoradylglycerol; PE: phosphatidylethanolamine; LysoPC: lysophosphatidylcholine; EA: ethanolamide.

The metabolites involved in the significant metabolic pathways altered obtained by Metaboanalyst at 28 days, have been represented in bar charts to visualize their response (fold change variation) along the exposure time (Fig. 7).

4. Discussion

4.1. Bioaccumulation

The determination of the different xenobiotics of the "chemical cocktail" reveals that As and Cd were mainly accumulated in hepatopancreas followed by gills and finally abdominal muscle (Fig. 1). This same trend was found in previous studies of crayfish *P. clarkii* captured in contaminated areas of southwestern Spain (Fernández-Cisnal et al., 2018; Gago-Tinoco et al., 2014). Previous studies have revealed that hepatopancreas could accumulate Cd in a time- and dose-dependent manner (Zhang et al., 2019). Results show that As concentration is predominant over Cd concentration in abdominal muscle and gills, which has been previously reported by other studies in *P. clarkii* (Anandkumar et al., 2020).

To our knowledge, there are not previous studies showing the bioaccumulation of metals after a depuration process. As can be seen in Fig. 1, As and Cd show a general tendency to increase the concentration throughout the exposure experience (21 days), while a decrease in the concentration of these elements is observed after 7 days of the

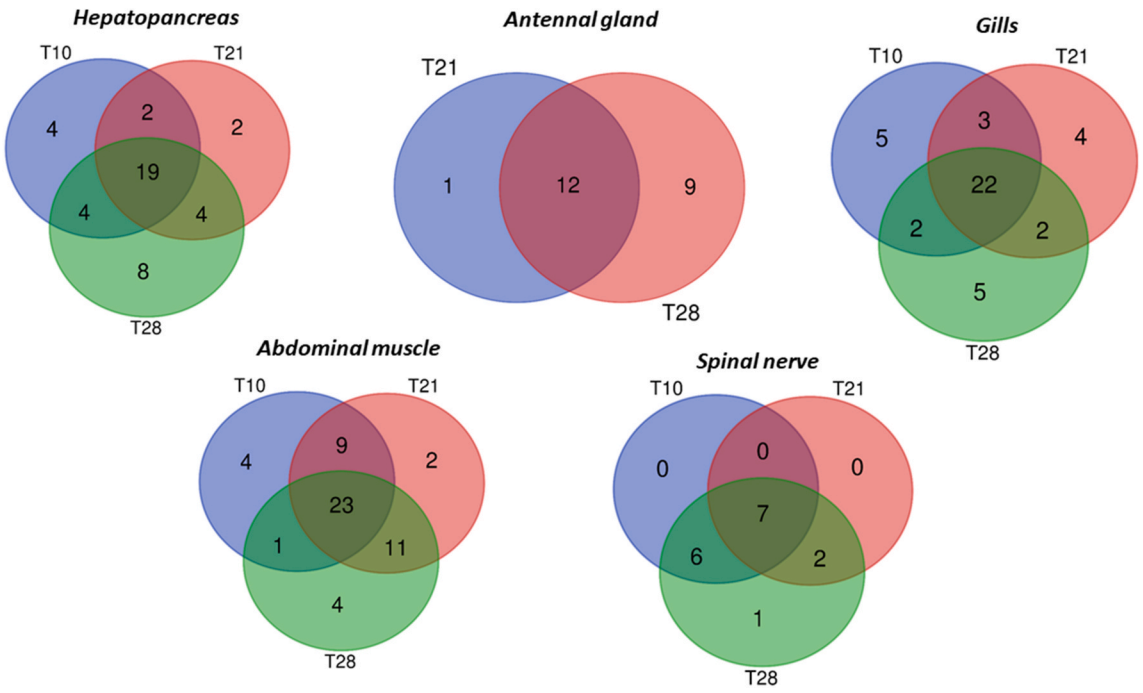

Fig. 4. Venn diagrams containing metabolites altered in each tissue analysed by UPLC-QTOF-MS and GC-MS at different days of the exposure.

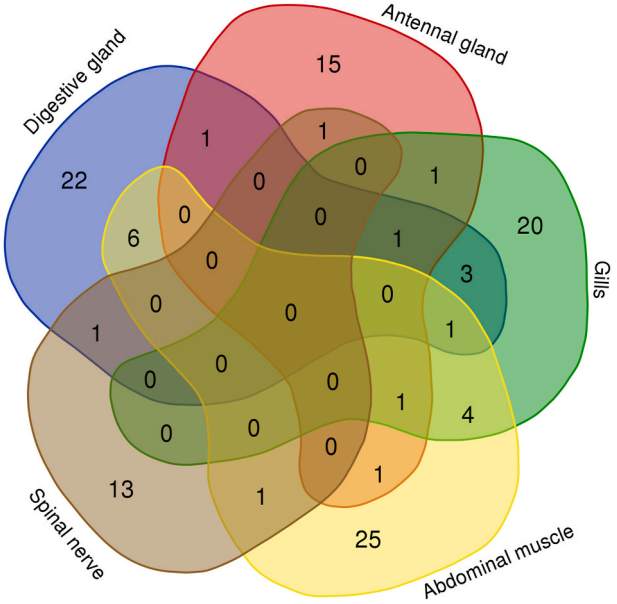

Fig. 5. Venn diagrams containing relevance metabolites in organs of *P. clarkii* crayfish after 28 days of exposure identified by UPLC-QTOF-MS and GC-MS.

depuration process. This can be observed in hepatopancreas, especially for As and for both metals in gills, where the levels decreased to those found control or even below. This is also the case in the abdominal muscle for Cd, but not for As, which increased the concentration in this tissue in the depuration phase.

Analysis of DCF concentration in both *P. clarkii* tissues and in the water tank strongly suggests that the crayfish controls the bioaccumulation process. We found a DCF concentration in the water 2–3 times higher than the nominal concentration on days 5–15, and this DCF could only result from crayfish excretion. DCF accumulation occurred in the abdominal muscle, but not in the hepatopancreas, with low bioconcentration factors. A high interindividual variability was found in the DCF amount detected in the abdominal muscle of exposed crayfish at the 10th day, ranging from undetected to 24.2 ng g^{-1} (w/w), indicating different capacity to cope with DCF. Interindividual variability decreased on successive days, but mean values remained relatively constant over time, even after the depuration period. The results obtained for water and tissues suggest that crayfish are able to regulate DCF accumulation in their tissues. However, we found that DCF was present in the abdominal muscle of *P. clarkii* after depuration and at a concentration similar/superior to that found in the previous days, suggesting that the strategy followed to accumulate and neutralize DCF turned out to be a double-edged sword that hampered its excretion. DCF can form complexes via chelation with certain metal ions (Lonappan et al., 2016) changing its properties, thus its association with metals could produce changes in the metabolism of the organisms exposed to a chemical cocktail containing metals and DCF, which could explain the similar behaviour in the bioaccumulation pattern of As. As previously commented, DCF was detected only in one hepatopancreas of one organism after 21 days of exposure. These results differ significantly from those obtained by other authors (Schwaiger et al., 2004) in fish, where very high levels of DCF were found in the liver after exposure, what might evidence the joined effect of the chemical cocktail exposure.

4.2. Biotransformation of DCF

In relation to the target metabolite screening, it is worth noting their low presence in the abdominal muscle samples at all exposure times studied. Of the 46 metabolites analysed (Table S11 for more details), only three metabolites were identified in the abdominal tissue samples. This is in stark contrast with the reports of other authors (Triebskorn et al., 2004) who identified up to nine metabolites in invertebrate samples. Specifically, in the samples analysed after 10 days of exposure only one sample out of five showed the presence of OH-DCF-dehydrogenated ($C_{14}H_9Cl_2NO_3$) with *m/z* 310,0038 (fragment 291.9953) at 6.44 min in positive polarity.

With regard to the samples at 21 days of exposition, only the presence of OH-DCF-dehydrogenated ($C_{14}H_9Cl_2NO_3$) with *m/z* 310.0038 (fragment 291.9953) at 6.48 min in positive polarity was observed in one sample out of the five specimens analysed. On the other hand,

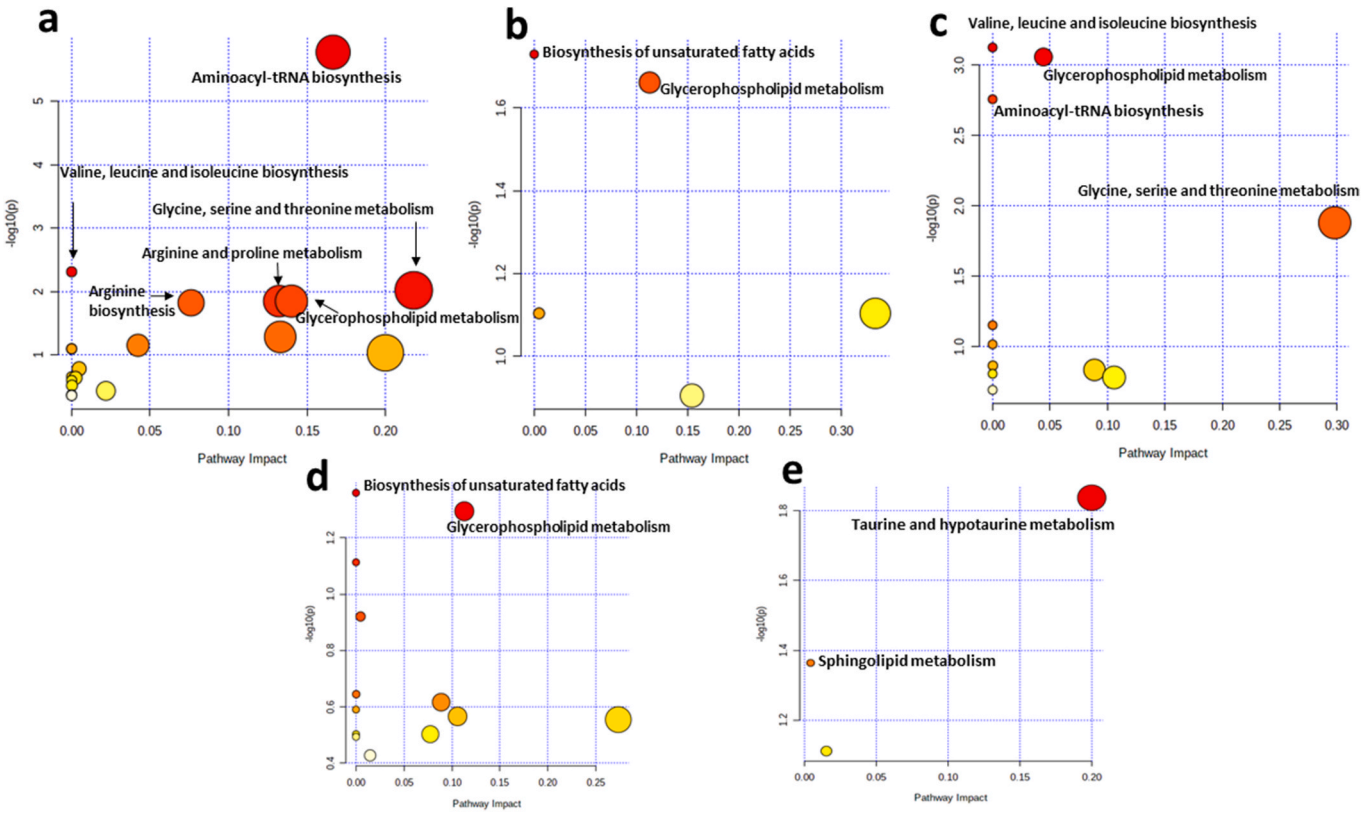

Fig. 6. Metabolome view map of significant metabolic pathways altered after 28 days of exposure to As, Cd and DCF in: a) hepatopancreas, b) antennal gland, c) gills, d) abdominal muscle and e) spinal nerve.

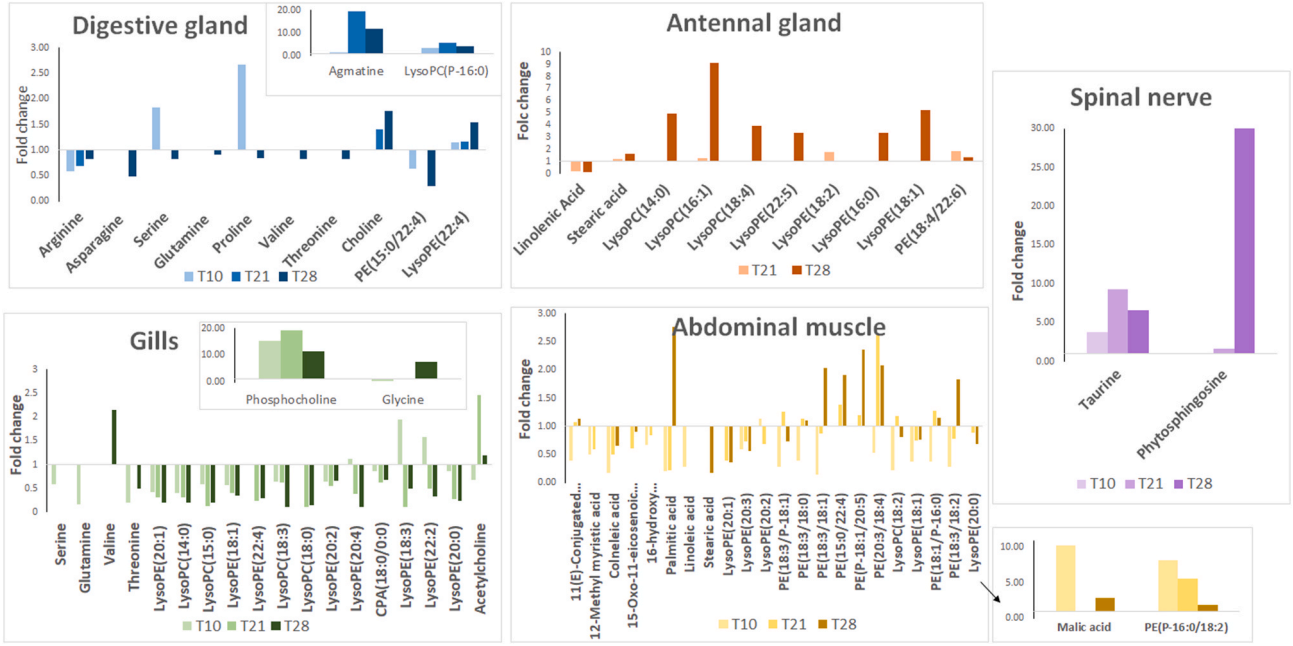

Fig. 7. Bar chart showing the fold changes of those metabolites involved in the significant metabolic pathways altered by the exposure to the "chemical cocktail" in each tissue (T28).

samples processed after 28 days gave positive results for hydroxyglucuronide indoline (Na^+) ($C_{20}H_{16}C_{l2}N_1O_8Na$) with *m/z* 492,0229 (fragment 175.1130) at 2.46 min and hydroxyglucuronide (Na+) ($C_{20}H_{18}C_{l2}N_1O_9Na$) at 13.63 min with *m/z* 510,0335 (fragment 175.1130).

In contrast, hepatopancreas showed the presence of 6 metabolites. Thus, in hepatopancreas analysed after 10 days the presence of a metabolite with *m/z* 376.0899 and retention time 5.5 was found in all exposed samples, main fragment ion in the fragment spectrum at 322.1635 was identified. This would match with the previously reported

metabolite 1-beta-O-acylglucuronide ($C_{20}H_{19}O_2N_1Cl_2$). The OH-DCF-dehydrogenated metabolite ($C_{14}H_9Cl_2NO_3$) with *m/z* 310.0038 (fragment 291.9953) at 6.40 min and methyl ester metabolite ($C_{15}H_{13}Cl_2NO_2$) with *m/z* 310.0244 (fragment 278.0150) at 6.94 min were also confirmed in three of the five specimens exposed.

The presence of the 3-OH and 4-OH-DCF (level of concentration < LOQ) was confirmed in 4 of the five specimens analysed, at 6.33 and 6.60 min respectively in samples collected after 21 days of exposition. Additionally, a metabolite with *m/z* 310.1348, initially assigned by Chromalynx as methyl ester, was also identified in all samples at 3.9 min. The deep analysis of the retention time and spectra, with fragments *m/z* 292.1221, 124.0071 did suspecting this metabolite corresponds to other DCF-derived structure not reported before.

In the samples collected at 28 days, only the metabolite 1-beta-O-acylglucuronide ($C_{20}H_{19}O_2N_1Cl_2$) with *m/z* 376.0870 and retention time 5.5 min was found, which would be in accordance with the depuration phase in which the animals were not feed the chemical cocktail.

The targeted analysis reveals the presence of DCF metabolites is higher in the hepatopancreas samples, with a higher number of metabolites found at higher exposure times, concretely at 21 days.

The metabolic transformation pathway that appears to be most recurrent involves hydroxylation and conjugation of DCF with glucuronic acid, this would be in contrast to reported by Qiuguo et al. in invertebrates, who found the most important metabolic transformation pathway to be the taurine conjugation of DCF. Accordingly, the metabolization of DCF and therefore its toxicity depends to a large extent not only on the species involved, but also on the conditions under which the drug is assimilated, so that, "chemical cocktails" may change the main biotransformation pathways of the animals exposed to, changing their metabolism.

4.3. Alteration of metabolic pathways

The untargeted metabolomic analysis reveals that the "chemical cocktail" induces the impairment of an important number of metabolites in each tissue along the exposure time. Hepatopancreas was the organ where a major number of metabolic pathways resulted affected, which could be explained by the fact that is an organ of great metabolic activity. However, other tissues revealed important metabolic impairments. In fact, the highest number of altered metabolites were found after 28 days of the exposure experiment in the abdominal muscle > hepatopancreas > gills > antennal glands > spinal nerve. As can be seen in Fig. 3, there is a band of metabolites that are considerably increased in hepatopancreas after 10 days of exposure (serine, malic acid, proline, glutamic acid and cholesterol), while other is clearly downregulated (*e.g.* choline, glucosphingosin, taurine, guanosine, glutamine PE (15:0/22:4), C16 sphinganine, phosphate, DG (20:2/22:5), MG (20:5), 3-eicosyne). After 21 days of exposure, the abundance of the first band is partially restored to the abundance of the control, but the second band decrease again, especially sarcosine, 3-eicosyne, PE (15:0/22:4), linalyl benzoate and chloroquine. After 7 days of depuration (T28), the trend is different and there are two new altered bands, one with overexpressed metabolites against the control (isoleucyl-threonin, MG (15:0), bentazole, choline, glucosylsphingosin, taurine, guanosine, guggulsterone) and other with downregulated metabolites (*e.g.* asparagine, valine, inosine, 2-hexenoylcholine, turanose, threonine).

The most altered pathways are commented in the following sections.

4.4. Glycerophosphoslipid metabolism

Pathway analysis showed alterations in the glycerophospholipid metabolism of the hepatopancreas, abdominal muscle, gills and antennal gland (Fig. 6). Increased abundance of phospholipids derivatives was found in hepatopancreas and antennal gland while a decrease was observed in the gills. Lysophosphatidylcholines (LPCs), components of plasma membranes, are converted to glycerolphosphocholines (GPCs), obtaining phosphocholine and choline as final products. The variation in the levels of these compounds shows oxidative stress due to the presence of As, Cd and DCF in *P. clarkii* crayfish (Fernández-Cisnal et al., 2018). In environmental metabolomic, oxidative stress has become an important issue to evaluate exposure to environmental or native stressors like pesticides, heavy metals, salinity values, temperature and others. In gills, we observed a general decreasing trend of the fold changes along the exposure time (higher downregulation in the exposed group and control group) (Table S6), which may indicate greater oxidative stress as the experience of exposure progresses. Moreover, phosphocholine has been found increased in gills which is a product of fragmentation of the plasma membranes (Table S6). Other authors have demonstrated that Cd induced oxidative stress and other disorder diseases in the hepatopancreas of *P. clarkii* (Zhang et al., 2019).

On the other hand, an increase in choline levels (1.40- and 1.77-fold at 21 and 28 days of exposure, respectively) was observed in the hepatopancreas (Table S4). Choline is part of the structure of the LPCs, which are major components of plasma membranes together with lysophosphatidylethanolamines (LPEs). The highest fold change values of choline were found in hepatopancreas.

4.5. Fatty acids metabolism

The analysis of metabolic pathways shows that biosynthesis of unsaturated fatty acid was significantly altered in antennal gland and abdominal muscle (Fig. 6).

Lipids are necessary compounds for the conservation of the tissue role, using as an important source of energy organisms. Linoleic acid and stearic acid were significantly downregulated in antennal gland (Table S5) and palmitic acid, linoleic acid, stearic acid,11-conjugated linoleic acid, 12-methyl myristic acid, colneleic acid, 15-oxo-11-eicosenoic acid and 16-hydroxy hexadecanoic acid were also downregulated in abdominal muscle (Table S7). Some fatty acids were also downregulated in the hepatopancreas, although they were not related with any significant pathway in Metaboanalyst (Fig. 6). This could indicate that As, Cd and DCF impair the biosynthesis of fatty acids or favour their degradation.

Other authors have shown similar alterations in some fatty acids in the crustacean *Daphnia magna* planktonic after Cd exposure (Taylor et al., 2010). In contrast, fatty acids were found over-expressed in the spinal nerve throughout the exposure experiment, especially after 28 days. The process of desaturation of fatty acid increases the amount of double bonds, originating some benefits to the membrane as fluidity and integrity, ion trafficking and improves the disorder of cellular functions (Mao et al., 2012).

4.6. Amino acid metabolism

Metabolic pathway analysis showed alterations in different routes affecting amino acids: (i) In hepatopancreas: aminoacyl-tRNA biosynthesis; valine, leucine and isoleucine biosynthesis; glycine, serine and threonine metabolism; arginine and proline metabolism; and arginine biosynthesis and (ii) in gills: aminoacyl-tRNA biosynthesis, valine, leucine and isoleucine biosynthesis, glycine, serine and threonine metabolism. Moreover, several amino acids were also altered in abdominal muscle (Table S7) at 10 and 21 days of exposure, but they were not significant after 28 days of exposure experiment, when the pathway analysis were performed.

A decrease in the level of several amino acids, such as asparagine, arginine, glutamine, serine, valine, threonine and proline, was found in different tissues of *P. clarkii* after As, Cd and DCF exposure. Numerous authors have demonstrated that exposure to pollutants can affect amino acid levels due to many toxic compounds can disturb osmoregulation, where they are used as the main osmolytes to equilibrate their intracellular osmolarity with outside environmental conditions (Viant,

2003). The results obtained are in agreement with previous results obtained by other authors, which reported down-regulated amino acid in a wide number of exposure experiments to metals, mainly in bivalves (Zhang et al., 2011).

4.7. Alterations in the levels of neurotransmitters

Our data shown increased levels of acetylcholine in gills in the exposed group after 21 and 28 days of exposure (Table S6). Acetylcholine, which is generated by choline acetyltransferase and then transformed to acetate and choline by the acetylcholinesterase enzyme, is an important neurotransmitter in nervous system, produced by enzyme. Our data are in good agreement with several studies that have demonstrated that the enzyme acetylcholinesterase is powerfully inhibited by numerous pollutants such as pesticides and metals, which causes accumulation of acetylcholine (Čolović, M.B et al., 2013). Moreover, acetylcholine performs a key function in several physiology activities such as the regulation of the inflammatory answer to prevent the morbidity and mortality of individuals (Fernández-Cisnal et al., 2018).

Taurine has been found increased in spinal nerve throughout the exposure experiment and after 28 days in hepatopancreas (Tables S8 and S4, respectively). This sulfonic acid, is involved in many important biological roles, like antioxidant activity, osmoregulation and membrane stabilization (Manna et al., 2009). This result is in agreement with the results obtained by other authors in aquatic invertebrates exposed to xenobiotics such as mercury (Cappello et al., 2015), copper (Liu et al., 2011) or niquel (Jones et al., 2008).

Finally, our results shown the association of As and Cd with metabolites as they can disturb a wide number of enzymes and metabolic pathways (Fig. S3) (Konz et al., 2017).

5. Conclusions

The combination of target and untargeted metabolomics allowed the decipherment of a large number of altered compounds of *P. clarkii* in response to a chemical cocktail. In this sense, results show that *P. clarkii* is a good bioindicator to be used in environmental pollution studies, especially environmental metabolomics. Pathway analysis showed alterations in *glycerophospholipid metabolism* in hepatopancreas, abdominal muscle, gills and antennal gland; *fatty acids metabolism* in antennal gland and abdominal muscle; *amino acid metabolism* in hepatopancreas and gills; and, *neurotransmitters* such as acetylcholine in gills and taurine in spinal nerve. In addition, data highlight the great potential of mass spectrometry to assess metabolic perturbations in living organisms under toxic agents. Finally, the study of various organs allowed us a deeper knowledge of the metabolic pathways affected in *P. clarkii* after As, Cd and DCF exposure.

Credit author statement

GRM: Validation, formal analysis, investigation, writing - Original Draft and writing - Review & Editing; CRH: Methodology, Validation, writing, investigation, formal analysis; SRA: Validation, formal analysis, investigation; NAM: Methodology, Validation, writing, investigation, formal analysis; JLGA: writing - Review & Editing; NA: Visualization, Writing- Reviewing and Editing; MABL: Conceptualization, writing-writing - Review & Editing, investigation, Project administration, funding acquisition and supervision; RFT: Conceptualization, Methodology, Validation, writing, investigation, formal analysis, Project administration, funding acquisition and supervision; TGB: Conceptualization, methodology, supervision, writing - original draft, -review and editing, project administration, funding acquisition.

Declaration of competing interest

The authors declare that they have no known competing financial interests or personal relationships that could have appeared to influence the work reported in this paper.

Acknowledgements

This work was supported by the coordinated projects PGC 2018-096608-B-C21 and PGC 2018-096608-B-C22 from the Spanish Ministry of Science and innovation (MCIN). (Generación del Conocimiento. MCIN/AEI/10.13039/501100011033/FEDER "Una manera de hacer Europa"). Authors are grateful to FEDER (European Community) for financial support, Grant UNHU13-1E-1611. Rodríguez-Moro, G. thanks to Plan Andaluz de Investigación, Desarrollo e Innovación (PAIDI 2020) and Fondo Social Europeo for a postdoctoral grant (DOC_01115). Authors are grateful to Servicio General de Investigación de Microanálisis, CENTRO DE INVESTIGACIÓN TECNOLOGÍA E INNOVACIÓN (CITIUS). Universidad de Sevilla, for the use of some of the chromatographic equipment. Funding for open access charge: Universidad de Huelva / CBUA.

Appendix A. Supplementary data

Supplementary data to this article can be found online at https://doi.org/10.1016/j.chemosphere.2021.133410.

References

Anandkumar, A., Li, J., Prabakaran, K., Xi Jia, Z., Leng, Z., Nagarajan, R., Du, D., 2020. Accumulation of toxic elements in an invasive crayfish species (Procambarus clarkii) and its health risk assessment to humans. J. Food Compos. Anal. 88, 103449. https://doi.org/10.1016/j.jfca.2020.103449.

Barreales-Suárez, S., Callejón-Mochón, M., Azoulay, S., Bello-López, M.Á., Fernández-Torres, R., 2018. Liquid chromatography quadrupole time-of-flight mass spectrometry determination of six pharmaceuticals in vegetal biota. Uptake study in Lavandula dentata. Sci. Total Environ. 622–623, 655–663. https://doi.org/10.1016/j.scitotenv.2017.11.244.

Begley, P., Francis-McIntyre, S., Dunn, W.B., Broadhurst, D.I., Halsall, A., Tseng, A., Knowles, J., Goodacre, R., Kell, D.B., 2009. Development and performance of a gas chromatography-time-of-flight mass spectrometry analysis for large-scale nontargeted metabolomic studies of human serum. Anal. Chem. 81, 7038–7046. https://doi.org/10.1021/ac9011599.

Bini, G., Santini, G., Chelazzi, G., 2015. Pre-exposure to cadmium or zinc alters the heart rate response of the crayfish Procambarus clarkii towards copper. Bull. Environ. Contam. Toxicol. 95, 12–17. https://doi.org/10.1007/s00128-015-1535-3.

Cappello, T., Maisano, M., Giannetto, A., Parrino, V., Mauceri, A., Fasulo, S., 2015. Neurotoxicological effects on marine mussel Mytilus galloprovincialis caged at petrochemical contaminated areas (eastern Sicily, Italy): 1H NMR and immunohistochemical assays. Comp. Biochem. Physiol. C Toxicol. Pharmacol. 169, 7–15. https://doi.org/10.1016/j.cbpc.2014.12.006.

Čolović, M.B., D Z, K., Lazarevic-Pasti, T.D., Bondzic, A., Vasic, V.M., 2013. Acetylcholinesterase inhibitors: pharmacology and toxicology. Curr. Neuropharmacol. 11, 315–335.

Devesa, V., Súñer, M.A., Lai, V.W.M., Granchinho, S.C.R., Vélez, D., Cullen, W.R., Martínes, J.M., Montoro, R., 2002. Distribution of arsenic species in the freshwater crustacean Procambarus clarkii. Appl. Organomet. Chem. 16, 692–700. https://doi.org/10.1002/aoc.374.

European Commission Regulation (EC) No 1907/2006.

Fernández-Cisnal, R., García-Sevillano, M.A., García-Barrera, T., Gómez-Ariza, J.L., Abril, N., 2018. Metabolomic alterations and oxidative stress are associated with environmental pollution in Procambarus clarkii. Aquat. Toxicol. 205, 76–88. https://doi.org/10.1016/j.aquatox.2018.10.005.

Fernández-Cisnal, R., García-Sevillano, M.A., Gómez-Ariza, J.L., Pueyo, C., López-Barea, J., Abril, N., 2017. 2D-DIGE as a proteomic biomarker discovery tool in environmental studies with Procambarus clarkii. Sci. Total Environ. 584–585, 813–827. https://doi.org/10.1016/j.scitotenv.2017.01.125.

Gago-Tinoco, A., González-Domínguez, R., García-Barrera, T., Blasco-Moreno, J., Bebianno, M.J., Gómez-Ariza, J.-L., 2014. Metabolic signatures associated with environmental pollution by metals in Doñana National Park using P. clarkii as bioindicator. Environ. Sci. Pollut. Res. Int. 21, 13315–13323. https://doi.org/10.1007/s11356-014-2741-y.

García-Barrera, T., Gómez-Ariza, J.L., González-Fernández, M., Moreno, F., García-Sevillano, M.A., Gómez-Jacinto, V., 2012. Biological responses related to agonistic, antagonistic and synergistic interactions of chemical species. Anal. Bioanal. Chem. 403, 2237–2253. https://doi.org/10.1007/s00216-012-5776-2.

García-Sevillano, M.Á., García-Barrera, T., Gómez-Ariza, J.L., 2015. Environmental metabolomics: biological markers for metal toxicity. Electrophoresis 36. https://doi.org/10.1002/elps.201500052.

García-Sevillano, M.A., García-Barrera, T., Navarro, F., Abril, N., Pueyo, C., López-Barea, J., Gómez-Ariza, J.L., 2015. Combination of direct infusion mass spectrometry

and gas chromatography mass spectrometry for toxicometabolomic study of red blood cells and serum of mice Mus musculus after mercury exposure. J. Chromatogr. B. Analyt. Technol. Biomed. Life Sci. 985, 75–84. https://doi.org/10.1016/j.jchromb.2015.01.029.

Gedik, K., Kongchum, M., DeLaune, R.D., Sonnier, J.J., 2017. Distribution of arsenic and other metals in crayfish tissues (Procambarus clarkii) under different production practices. Sci. Total Environ. 574, 322–331. https://doi.org/10.1016/j.scitotenv.2016.09.060.

Hines, A., Staff, F.J., Widdows, J., Compton, R.M., Falciani, F., Viant, M.R., 2010. Discovery of metabolic signatures for predicting whole organism toxicology. Toxicol. Sci. 115, 369–378. https://doi.org/10.1093/toxsci/kfq004.

Hodson, P.V., 2002. Biomarkers and Bioindicators in monitoring and assessment. In: Adams, S.M. (Ed.), Biological Indicators of Aquatic Ecosystems Stress. American Fisheries Society, Maryland, U.S.A., pp. 591–619

Huner, J.V., 1988. Status of crayfish transplantations. Freshw. Crayfish 7, 29–34.

Izral, N.M., Brua, R.B., Culp, J.M., Yates, A.G., 2018. Developing metabolomics-based bioassessment: crayfish metabolome sensitivity to food and dissolved oxygen stress. Environ. Sci. Pollut. Res. 25, 36184–36193. https://doi.org/10.1007/s11356-018-3518-5.

Jones, O., Dondero, F., Viarengo, A., Griffin, J., 2008. Metabolic profiling of Mytilus galloprovincialis and its potential applications for pollution assessment. Mar. Ecol. Prog. Ser. 369, 169–179. https://doi.org/10.3354/meps07654.

Kazakova, J., Fernández-Torres, R., Ramos-Payán, M., Bello-López, M., 2018. Multiresidue determination of 21 pharmaceuticals in crayfish (Procambarus clarkii) using enzymatic microwave-assisted liquid extraction and ultrahigh-performance liquid chromatography-triple quadrupole mass spectrometry analysis. J. Pharm. Biomed. Anal. 160, 144–151. https://doi.org/10.1016/j.jpba.2018.07.057.

Konz, T., Migliavacca, E., Dayon, L., Bowman, G., Oikonomidi, A., Popp, J., Rezzi, S., 2017. ICP-MS/MS-Based ionomics: a validated methodology to investigate the biological variability of the human ionome. J. Proteome Res. 16, 2080–2090.

Kuehnbaum, N.L., Britz-Mckibbin, P., 2013. New advances in separation science for metabolomics: resolving chemical diversity in a post-genomic era. Chem. Rev. 113, 2437–2468. https://doi.org/10.1021/cr300484s.

Liu, X., Zhang, L., You, L., Yu, J., Cong, M., Wang, Q., Li, F., Li, L., Zhao, J., Li, C., Wu, H., 2011. Assessment of clam ruditapes philippinarum as heavy metal bioindicators using NMR-based metabolomics. Clean 39, 759–766. https://doi.org/10.1002/clen.201000410.

Lonappan, L., Brar, S.K., Das, R.K., Verma, M., Surampalli, R.Y., 2016. Diclofenac and its transformation products: environmental occurrence and toxicity - a review. Environ. Int. 96, 127–138. https://doi.org/10.1016/j.envint.2016.09.014.

Manna, P., Sinha, M., Sil, P.C., 2009. Taurine plays a beneficial role against cadmium-induced oxidative renal dysfunction. Amino Acids 36, 417–428.

Mao, Z.X., Fu, H., Nan, Z.B., Wang, J., Wan, C.G., 2012. Fatty acid content of common vetch (Vicia sativa L.) in different regions of Northwest China. Biochem. Systemat. Ecol. 44, 347–351. https://doi.org/10.1016/j.bse.2012.06.021.

Memmert, U., Peither, A., Burri, R., Weber, K., Schmidt, T., Sumpter, J.P., Hartmann, A., 2013. Diclofenac: new data on chronic toxicity and bioconcentration in fish. Environ. Toxicol. Chem. 32, 442–452. https://doi.org/10.1002/etc.2085.

Pasikanti, K.K., Ho, P.C., Chan, E.C.Y., 2008. Gas chromatography/mass spectrometry in metabolic profiling of biological fluids. J. Chromatogr. B Anal. Technol. Biomed. Life Sci. 871, 202–211. https://doi.org/10.1016/j.jchromb.2008.04.033.

Rodríguez-Moro, G., Roldán, F.N., Baya-Arenas, R., Arias-Borrego, A., Callejón-Leblic, B., Gómez-Ariza, J.L., García-Barrera, T., 2020. Metabolic impairments, metal traffic, and dyshomeostasis caused by the antagonistic interaction of cadmium and selenium using organic and inorganic mass spectrometry. Environ. Sci. Pollut. Res. 27, 1762–1775. https://doi.org/10.1007/s11356-019-06573-1.

Schwaiger, J., Ferling, H., Mallow, U., Wintermayr, H., Negele, R.D., 2004. Toxic effects of the non-steroidal anti-inflammatory drug diclofenac. Part I: histopathological alterations and bioaccumulation in rainbow trout. Aquat. Toxicol. 68, 141–150. https://doi.org/10.1016/j.aquatox.2004.03.014.

Suárez-Serrano, A., Alcaraz, C., Ibáñez, C., Trobajo, R., Barata, C., 2010. Procambarus clarkii as a bioindicator of heavy metal pollution sources in the lower Ebro River and Delta. Ecotoxicol. Environ. Saf. 73, 280–286. https://doi.org/10.1016/j.ecoenv.2009.11.001.

Sumner, L.W., Amberg, A., Barrett, D., Beale, M.H., Beger, R., Daykin, C.A., Fan, T.W.-M., Fiehn, O., Goodacre, R., Griffin, J.L., Hankemeier, T., Hardy, N., Harnly, J., Higashi, R., Kopka, J., Lane, A.N., Lindon, J.C., Marriott, P., Nicholls, A.W., Reily, M. D., Thaden, J.J., Viant, M.R., 2007. Proposed minimum reporting standards for chemical analysis: chemical analysis working group (CAWG) metabolomics Standards initiative (MSI). Metabolomics 3, 211–221. https://doi.org/10.1007/s11306-007-0082-2.

Taylor, N.S., Weber, R.J.M., White, T.A., Viant, M.R., 2010. Discriminating between different acute chemical toxicities via changes in the daphnid metabolome. Toxicol. Sci. 118, 307–317. https://doi.org/10.1093/toxsci/kfq247.

Triebskorn, R., Casper, H., Heyd, A., Eikemper, R., Köhler, H.R., Schwaiger, J., 2004. Toxic effects of the non-steroidal anti-inflammatory drug diclofenac: Part II. Cytological effects in liver, kidney, gills and intestine of rainbow trout (Oncorhynchus mykiss). Aquat. Toxicol. 68, 151–166. https://doi.org/10.1016/j.aquatox.2004.03.015.

Trombini, C., Kazakova, J., Montilla-López, A., Fernández-Cisnal, R., Hampel, M., Fernández-Torres, R., Bello-López, M.Á., Abril, N., Blasco, J., 2021. Assessment of pharmaceutical mixture (ibuprofen, ciprofloxacin and flumequine) effects to the crayfish Procambarus clarkii: a multilevel analysis (biochemical, transcriptional and proteomic approaches). Environ. Res. 200 https://doi.org/10.1016/j.envres.2021.111396.

Van Genderen, E., Adams, W., Dwyer, R., Garman, E., Gorsuch, J., 2015. Modeling and interpreting biological effects of mixtures in the environment: introduction to the metal mixture modeling evaluation project. In: Environmental Toxicology and Chemistry, pp. 721–725.

Viant, M.R., 2003. Improved methods for the acquisition and interpretation of NMR metabolomic data. Biochem. Biophys. Res. Commun. 310, 943–948. https://doi.org/10.1016/j.bbrc.2003.09.092.

Wei, K., Wei, Y., Song, C., 2020. The response of phenoloxidase to cadmium-disturbed hepatopancreatic immune-related molecules in freshwater crayfish Procambarus clarkii. Fish Shellfish Immunol. 99, 190–198. https://doi.org/10.1016/j.fsi.2020.02.012.

Wilson, C.E., Dickie, A.P., Schreiter, K., Wehr, R., Wilson, E.M., Bial, J., Scheer, N., Wilson, I.D., Riley, R.J., 2018. The pharmacokinetics and metabolism of diclofenac in chimeric humanized and murinized FRG mice. Arch. Toxicol. 92, 1953–1967. https://doi.org/10.1007/s00204-018-2212-1.

Xiong, Z., Weng, Y., Lang, L., Ma, S., Zhao, L., Xiao, W., Wang, Y., 2018. Tissue metabolomic profiling to reveal the therapeutic mechanism of reduning injection on LPS-induced acute lung injury rats. RSC Adv. 8, 10023–10031. https://doi.org/10.1039/c7ra13123b.

Zhang, L., Liu, X., You, L., Zhou, D., Wu, H., Li, L., Zhao, J., Feng, J., Yu, J., 2011. Metabolic responses in gills of Manila clam Ruditapes philippinarum exposed to copper using NMR-based metabolomics. Mar. Environ. Res. 72, 33–39. https://doi.org/10.1016/j.marenvres.2011.04.002.

Zhang, Y., Li, Z., Kholodkevich, S., Sharov, A., Chen, C., Feng, Y., Ren, N., Sun, K., 2020. Effects of cadmium on intestinal histology and microbiota in freshwater crayfish (Procambarus clarkii). Chemosphere 242, 125105. https://doi.org/10.1016/j.chemosphere.2019.125105.

Zhang, Y., Li, Z., Kholodkevich, S., Sharov, A., Feng, Y., Ren, N., Sun, K., 2019. Cadmium-induced oxidative stress, histopathology, and transcriptome changes in the hepatopancreas of freshwater crayfish (Procambarus clarkii). Sci. Total Environ. 666, 944–955. https://doi.org/10.1016/j.scitotenv.2019.02.159.

Zhang, Y., Sun, K., Li, Z., Chai, X., Fu, X., Kholodkevich, S., Kuznetsova, T., Chen, C., Ren, N., 2021. Effects of acute diclofenac exposure on intestinal histology, antioxidant defense, and microbiota in freshwater crayfish (Procambarus clarkii). Chemosphere 263, 128130. https://doi.org/10.1016/j.chemosphere.2020.128130.